

Quantum tunnelling without a barrier

Anne Weber, Margarita Khokhlova, and Emilio Pisanty

Attosecond Quantum Physics Laboratory, King's College London, London WC2R 2LS, UK

(Dated: November 24, 2023)

Tunnelling is a renowned concept in modern physics that highlights the peculiarity of non-classical dynamics. Despite its ubiquity questions remain. We focus on tunnelling through the barrier created by a strong laser field that illuminates an atomic target, which is essential to the creation of attosecond pulses and ultimately all attosecond processes. Here, we present an optical tunnelling event that, unexpectedly, happens at a time when the instantaneous electric field is zero and there is no barrier. We discover this strong-field ionisation event by introducing the colour-switchover technique – the gradual replacement of a laser field with its second harmonic – within which the zero-field tunnelling appears when the two amplitudes are equal. This event is a topologically stable feature and it appears at all Keldysh parameters. The tunnelling without a barrier highlights the disconnect between the standard intuition built on the picture of a quasi-static barrier, and the nonadiabatic nature of the process. Our findings provide a key ingredient to the understanding of strong-field processes, such as high-harmonic generation and laser-induced electron diffraction, driven by the increasingly accessible class of strongly polychromatic light fields.

The quantum-mechanical tunnel effect is an emblematic example of the peculiar and counter-intuitive behaviour of quantum particles, which can ‘tunnel’ through a potential-energy barrier that classical physics would deem impassable. Although the discovery of tunnelling dates back almost a century [1], there are still many open questions, such as how to experimentally measure the time the particle spends under the barrier [2, 3].

In nonlinear optics, tunnelling appears in the context of strong fields, in which the illuminating laser field is strong enough to distort the atomic Coulomb potential. The barrier created by the combination of the atomic and optical potentials allows the electron to escape from the atom [4] (see Fig. 1(a)). In this work, we present strong-field ionisation events for an atom subjected to a bichromatic laser field, and report on a nonadiabatic tunnelling event which, counter-intuitively, happens at a time when the instantaneous electric field is zero (see Fig. 1(b)).

Ionisation by strong laser fields is fundamental for the whole field of attosecond science, which aims at probing electronic and nuclear motion on its natural timescale using light pulses of attosecond duration [5]. The two major physical effects are above-threshold ionisation (ATI) [6, 7] and high-harmonic generation (HHG). In ATI, the photoelectron momentum distributions of the freed electrons are captured to give information about the electronic structure of the target. The process of HHG is understood in terms of three steps: strong-field ionisation, propagation in the laser field and recombination with the parent ion, upon which an attosecond pulse is emitted [8–10]. Hence, full control of the created attosecond pulses requires a reliable understanding of the process of strong-field ionisation.

The interaction of intense ultrashort laser pulses with matter is most commonly described using the strong-field approximation (SFA) [7, 11]. Following the works of Keldysh, Faisal, Reiss (KFR) and Peremolov et al. [12–15] the total ionisation yield in such an oscillating laser field is linked to the tunnelling rate in a static electric field, and hence, a static barrier. Within the SFA, ionisation is described in terms of discrete events in time which are identified by saddle points of the electron’s complex

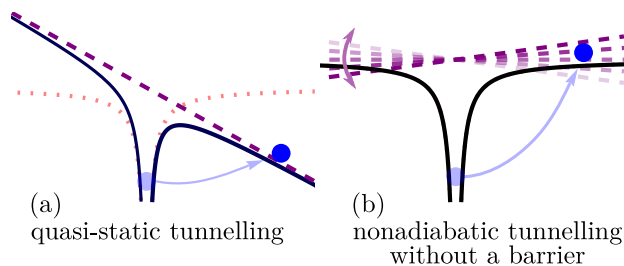


FIG. 1. Schematic view of field-induced tunnelling with the laser field’s vector potential, the atomic binding potential and the resulting barrier in the (a) quasi-static and (b) nonadiabatic regime in which the laser field changes during the process.

action. This formalism gives rise to the well-established and intuitive picture of quantum orbits [16, 17], and implies that ionisation is most likely to happen when the field is at its maximum.

In recent years, advances in light generation and measurement techniques allow (and ask) for a more detailed description of the strong-field tunnel ionisation process. Numerous studies focus on the nonadiabaticity of the phenomenon, taking into account the dynamics of the barrier [18–22], as well as the effects of the Coulomb potential on the various stages of the tunnelling process [23, 24]. For example, nonadiabatic effects are essential for the interpretation of tunnelling times in the so-called attoclock technique [25–31].

One of the key tools to investigate nonadiabatic effects are tightly controlled ‘tailored’ polychromatic drivers. Perturbative second-colour fields are often used as a temporal gate for the ionisation process and to control the harmonic signal [32–36]. Furthermore, strongly polychromatic drivers, where the two combined fields have similar amplitudes, have become experimentally feasible and are increasingly popular in attosecond science. They allow for a versatile shaping of the harmonic radiation both in intensity and polarisation, and thus offer control over the main features of the emitted attosecond pulse [37–41]. Generic polychromatic drivers are there-

fore necessary to build a comprehensive understanding of the strong-field processes, starting from their first step – tunnelling.

In this letter we present a tunnel ionisation event that happens in a two-colour strong-field setup at a time when the instantaneous electric field is zero and hence there is no barrier. This counter-intuitive finding arises as part of the colour switchover, which describes the continuous tuning from a monochromatic linearly polarised driving laser field to its second harmonic. The discrete tunnel ionisation events are analysed in terms of saddle points of the semi-classical action, using the strong-field approximation. We present how each ionisation event contributes to the final spectrum, as well as the respective quasi-classical trajectories of the direct photoelectrons. We show how the results scale with the wavelength, and can ultimately conclude that the ionisation event that happens at zero field is a topologically stable feature of the strongly bichromatic field. The tunnelling event that happens without a barrier has a weak, but non-zero contribution to the spectrum, which emphasizes the need for further explanation of the under-the-barrier dynamics. Moreover, experimental observables that show the significance of this event have yet to be found.

To this end, we consider ATI within the SFA approach. The ionisation amplitude in atomic units for a given final (drift) momentum p is described by the integral [42]

$$\Psi(p) = \int_{-\infty}^{\infty} \mathcal{P}(p + A(t)) e^{-iS(p,t)} dt \quad (1)$$

with the semi-classical action

$$S(p, t) = \int_{-\infty}^t \left[\mathcal{I}_p + \frac{1}{2} (p + A(t'))^2 \right] dt'. \quad (2)$$

Here, the vector potential of the driving laser field is $A(t) = -\int E(t) dt$, and the slowly varying prefactor $\mathcal{P}(k) = i(\mathcal{I}_p + k^2/2) \varphi_0(k)$ encodes information about the dipole moment with ground state φ_0 and ionisation potential \mathcal{I}_p . Employing the saddle-point method then reduces the integral (1) to a summation of contributions at the stationary points of the action [43–45]. Those saddle points t_s are given by

$$\frac{\partial S}{\partial t}(p, t_s) = 0, \quad (3)$$

are in general complex numbers, topologically conserved and ultimately correspond to the discrete ionisation events within one laser cycle.

The saddle-point method is the established approach for scenarios in the strong-field tunnelling regime due to its unique combination of intuition and quantitative modelling. It rigorously links the mathematically strict formalism of saddle points to the intuitive picture of discrete ionisation events which then lead to distinguishable quantum orbits. In the following we apply it to the colour-switchover scenario.

We suggest the colour switchover as a simple and essential technique for understanding strong-field physics with strongly polychromatic drivers. We consider a linearly polarised laser field which is gradually replaced by

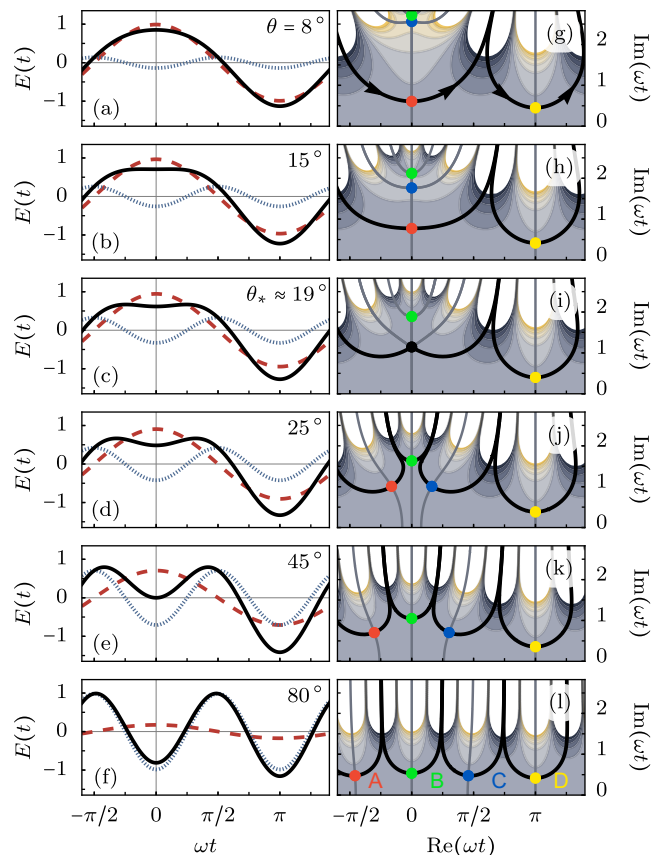


FIG. 2. Left column: Total waveform of the bichromatic field (4) (black solid line) and of its components (ω -field: red dashed, 2ω -field: blue dotted) throughout the colour switchover performed by increasing the mixing angle θ from 8° , through 15° , $\theta_* \approx 19^\circ$, 25° , 45° to 80° , (a-f) respectively. Right column: $\text{Im}(S(p=0, t))$ over the complex ωt -plane (g-l) for the fields presented on the left and $\mathcal{I}_p = 0.5$. Stationary points ωt_s are highlighted by coloured dots and are referred to by their labels shown in panel (l). Their contour lines for constant real action are drawn as grey lines, with the resulting integration contour in black.

its second harmonic, such that the resulting electric field can be understood as a two-colour field where we increase the amplitude ratio between the ω and the 2ω component, while keeping the total intensity constant. That is, the total electric field is given by

$$E(t) = E_1 \cos(\omega t) - E_2 \cos(2\omega t) \quad (4)$$

with the amplitudes $E_1 = E_0 \cos \theta$ and $E_2 = E_0 \sin \theta$ defining the mixing angle $0^\circ \leq \theta \leq 90^\circ$, which corresponds to tuning the amplitude ratio $R = E_2/E_1 = \tan(\theta)$ from 0 to infinity. The two constituent fields and their superposition (4) are shown in the left column of Fig. 2 for several values of θ , demonstrating the colour switchover.

This scenario is of special interest because the number of contributing saddle points, i.e., the number of discrete ionisation events, per cycle of the fundamental $2\pi/\omega$ changes. Clearly, for the ω -dominated field there are two ionisation events per cycle, namely at $\text{Re}(\omega t) = 0$ and π in Fig. 2(a), whereas for the 2ω -dominated field there are four ionisation events per cycle, at around

$\text{Re}(\omega t) = -\pi/2, 0, \pi/2$ and π in Fig. 2(f). As saddle points are topologically protected mathematical objects, and therefore stable features of the system, this colour switchover raises a number of core questions:

- Where do the new ionisation events come from?
- When do they start to contribute?
- Where do they go?
- Which are the new ones and which are the old ones?

Answering those questions is nontrivial and requires a rigorous mathematical approach. An often neglected part of applying the saddle-point method (also called method of steepest descent) to the integral (1) is that the summation does not include all saddle points t_s of the action (2), but only those which are part of a valid integration path. There typically exist numerous solutions to (3) from which we need to select the ones which are contained in the steepest-descent route. In the right column of Fig. 2 we therefore present contour maps of the imaginary part of the action over complex time for the fields on the left column of Fig. 2. We use a total incoming intensity $I_0 = E_0^2 = 4 \times 10^{14}$ W/cm², fundamental frequency $\omega = 0.057$ a.u. ($\lambda = 800$ nm), zero drift momentum, and a hydrogen target ($\mathcal{I}_p = 0.5$ a.u.). The saddle points and their respective level lines are highlighted with grey solid lines and the resulting integration contour is shown in black.

As one might expect, in the early stage of the colour switchover the integration contour only passes through two saddle points, which we call A (red) and D (yellow). We find additional saddle points B (green) and C (blue) coming in from high imaginary parts in Fig. 2(g) and (h), but they are not yet part of the integration contour and hence do not yet contribute to the ionisation amplitude. As we subsequently increase the amplitude ratio they move closer towards the real axis and C eventually coalesces with the ‘old’ saddle point A to one second-order saddle point as shown in Fig. 2(i). The point where the coalescence happens is at $\theta \approx 19^\circ$ and we denote it by $\theta_* \equiv \arctan(R_*)$. For the rest of the switchover, the three saddle points A , B and C move apart until they spread out evenly parallel to the real axis (Figs. 2(j-l)). In Fig. 2(l) we find the expected structure of four evenly spaced ionisation events A , B , C and D for the almost-monochromatic 2ω -field shown in Fig. 2(f).

In general, how and when the saddle points B and C enter the integration contour depends on the drift momentum. Considering saddle points for non-zero drift momentum p yields a more complicated manifold of solutions in which the coalescence marks a unique branch point that will be dealt with in a future publication. Here, we focus on the special case of zero momentum because therein saddle point B corresponds to the tunnelling event that eventually happens without a barrier.

Strictly speaking, whenever two saddle points coalesce, or are in close proximity, the saddle-point method breaks down. Approximating the integral (1) then requires higher-order methods, such as uniform expansions [46], which for our case are complicated by the presence of the third saddle point. A more detailed exploration follows in

an upcoming publication. The coalescence at $R_* \approx 0.36$ marks the amplitude ratio following which the ‘new’ saddle points B and C are part of the integration contour. That is, for all amplitude ratios above R_* the new saddle points (along with A and D) indubitably contribute to the total ionisation amplitude.

Consider that this change in number of contributing saddle points happens surprisingly early within in the colour switchover. Let us focus on the saddle point B , which is at $\text{Re}(\omega t) = 0$. Examining the electric field at $t = 0$ we find that it marks a contributing ionisation event even before the electric field has changed sign ($E(0) > 0$, as in Fig. 2(d)) and therefore implies tunnelling uphill. Most importantly, and as advertised, this tunnel ionisation event also contributes to the total ionisation amplitude at the point at which the electric field is zero ($E(0) = 0$, Fig. 2(e)) and there is in fact no barrier formed (Fig. 2(k), saddle point B at $\omega t \approx 0 + 1.1i$).

This finding is deeply surprising when thinking of strong-field ionisation in terms of the well-established two-step model derived from the quasi-static intuition. One possible explanation is to take into account the nonadiabaticity of the process using the complex-time model explained in [44]. Thereupon the saddle point t_s marks the moment the electron enters the barrier, wherein the imaginary part is understood as the time the electron spends under the barrier, and the real part is the moment it appears in the continuum (read: exits the barrier). As, in our case, the electric field is non-zero during that tunnelling time, i.e., for the time between t_s and $\text{Re}(t_s)$, one could argue that there is a barrier formed which allows the electron to tunnel. However, the dynamics in imaginary time in this case are still unclear.

For non-zero momenta the situation is essentially the same as for $p = 0$. As the field shape depends smoothly on the mixing angle, for any given drift momentum we can always find an ionisation event happening at a time when the electric field is zero. We illustrate this using the following vice-versa consideration. For the situation of equal amplitudes of ω and 2ω -field ($R = 1$) the ionisation time depends smoothly on the momentum. Hence, for a small positive (negative) drift momentum the ionisation happens shortly before (after) the field extremum. For the spanned ionisation window around $t = 0$ the electric field is then non-zero. However, inspecting Fig. 2(e) shows that the respective instantaneous field amplitude ultimately is still comparatively low and leaves us surprised about the existence of an ionisation event.

To further expand on the intuitive understanding of the ionisation events, we show the electrons’ displacement in the electric field given by

$$x(t) = \int_{t_s}^t (p + A(t')) dt'. \quad (5)$$

The temporal integration here follows a two-legged contour in the complex plane, starting from the complex-valued saddle point $t = t_s$ downwards to the real axis [44, 47, 48]. From $t = \text{Re}(t_s)$ onwards, the integration is carried out along the real axis. In Fig. 3 we show the resulting semi-classical trajectories for all four ionisation events shown in Fig. 2(l), and also indi-

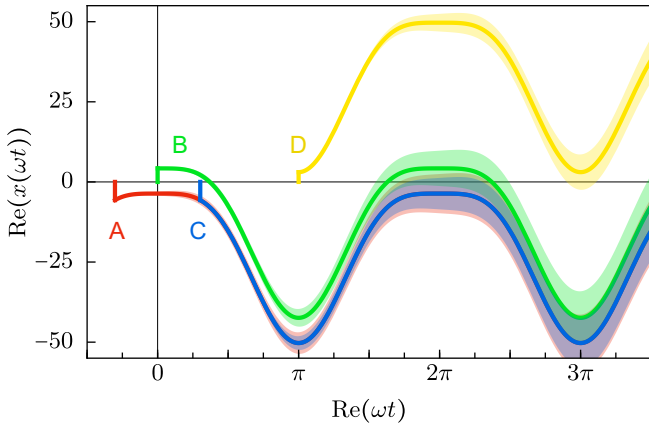


FIG. 3. Semi-classical trajectories (5) for the field with the four labelled ionisation events shown in Fig. 2(e). The semi-transparent bands show the trajectories for solutions with $|p| < 0.05$.

cate the trajectories for solutions with non-zero momentum. In general, the displacement at the tunnel exit $x_{\text{exit}} = \text{Re}[x(\text{Re}(t_s))]$ is non-zero for all trajectories, which confirms that the electrons are indeed freed via tunnel ionisation. Upon appearance in the continuum we find that the trajectories stemming from ionisation events C and D are led away from the core, as expected. By contrast, electrons freed in ionisation events A and in particular B are driven back towards the core. In general, we find that upon their return all three trajectories A , B and C remain in the core's vicinity for a significant fraction of the cycle (at around $\omega t \approx 2\pi$). These trajectories are therefore highly susceptible to Coulomb effects. As explained above, the ionisation event at zero field is a stable feature of the colour switchover and remains even for arbitrary phase shifts between the two constituent fields. We could choose the location of the zero-field tunnelling event such that the effects of the Coulomb forces are minimised. However, our primary interest is to show the existence of a tunnel ionisation event, within the SFA framework, that happens at a time when there is no barrier.

We now turn to the contribution of each ionisation event to the total ionisation amplitude. Applying the saddle-point method (SPM) to the SFA integral (1) results in a summation over the discrete ionisation events that are part of the integration contour shown in the right column of Fig. 2:

$$\begin{aligned} \Psi_{\text{SPM}}(p) &\approx \sum_s \Psi_{\text{SPM}}^s(p) \\ &= \sum_s \sqrt{\frac{2\pi}{iS''}} \mathcal{P}(p + A(t)) e^{-iS(p, t_s)}. \end{aligned} \quad (6)$$

For the atomic target we assume a hydrogenic short-range potential such that $\mathcal{P}(k) = i/\sqrt{\pi} (2\mathcal{I}_p)^{\frac{1}{4}}$. We are especially interested in the contribution of the zero-field ionisation event, B . Hence, in Fig. 4(a) we show the spectrum $|\Psi_{\text{SPM}}(p)|$ (black) for the field shown in Fig. 2(e), with the contributions of each ionisation event s

in Fig. 2(k). We find that the contribution of this specific ionisation event is small compared to that of A and C , and particularly D . In fact, for the majority of the colour switchover (field shapes as in Figs. 2(c-f)) the spectrum is clearly dominated by the contribution of D such that the contribution of orbit B is hidden below the others and does not have an observable effect. This becomes obvious when we recall that the ionisation for orbit D happens when the instantaneous field amplitude is largest (around $\text{Re}(\omega t) \approx \pi$, see Fig. 2 left column), and that the instantaneous electric field enters exponentially into the ionisation amplitude via the action (2).

Because the theoretical SFA framework connects to, and is often benchmarked against, the quasi-static theory, we explore how the relevance of the zero-field tunnelling event changes as we approach the adiabatic limit. For that, in Fig. 4(b) we present each orbit's integrated contribution to the spectrum,

$$Y_s = \int |\Psi_{\text{SPM}}^s(p)|^2 dp, \quad (7)$$

for various Keldysh adiabaticity parameters $\gamma = \sqrt{\mathcal{I}_p/2U_p}$. The ponderomotive energy U_p for the equal-amplitudes field configuration of Fig. 2(e) is $\gamma = 4\omega\sqrt{\mathcal{I}_p/5I_0}$. We keep \mathcal{I}_p and I_0 constant such that the displayed range of Keldysh parameters corresponds to wavelengths $330 \text{ nm} \leq \lambda \leq 3000 \text{ nm}$. From the quasi-static limit ($\gamma \ll 1$) to the multi-photon ionisation regime ($\gamma > 1$), the orbit D dominates the spectrum, followed by A and C , which contribute equally. Their relative contribution remains almost unchanged across the range of Keldysh parameters. In contrast, we find that the contribution of orbit B decreases as we approach the quasi-static regime. Note, that the electric field is zero at $t = 0$ independently of the Keldysh parameter and for the considered range always hosts a contributing saddle point as well. Ultimately, the tunnelling event at zero field loses significance for the total spectrum as we move towards the adiabatic limit. Although this matches our quasi-static intuition and is somewhat reassuring, we want to emphasize that the experimentally relevant parameters above result in $\gamma = 0.67$. Thus, within the realms of typical configurations like ours, the contribution of orbit B must not be ignored.

With the change of driving laser field parameters it is essential to ask if the tunnelling event without a barrier remains a contributor to the total ionisation amplitude in the quasi-static limit. That is, we need to verify whether the saddle point B , which for $R = 1$ corresponds to the tunnelling without barrier is always part of the integration contour even if the wavelength changes. As explained earlier, for a given configuration, the saddle point B (as well as C) needs to be taken into account from the coalescence point R_* on, i.e., for all amplitude ratios $R > R_*$. In Fig. 5 we show that the amplitude ratio R_* decreases monotonically with the Keldysh parameter (solid line). The dependence can be well approximated by the asymptotes $1 - \sqrt[3]{135/32} \gamma^{\frac{3}{2}}$ in the small-wavelength limit and by $1/4\gamma$ in the long-wavelength limit (dashed and dotted lines respectively). Most importantly, Fig. 5 shows that the saddle point B for $R = 1$ is part of the

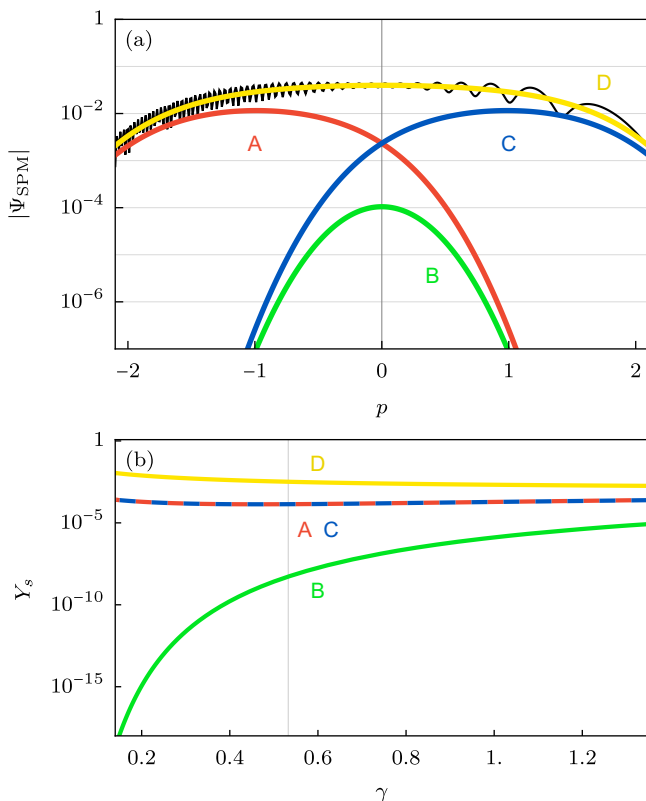


FIG. 4. (a) Magnitude of the spectral ionisation amplitude $|\Psi_{\text{SPM}}|$ (black), and the contribution $|\Psi_{\text{SPM}}^s|$ of each of the four contributing ionisation events shown in Fig. 2(k) for atomic hydrogen ionised by the field in Fig. 2(e). For $p = 0$, the contribution B (green) stems from the ionisation event at zero field. (b) Scaling of the total ionisation amplitude per orbit Y_s for a field shaped like the one shown in Fig. 2(e), for a range of Keldysh parameters γ . Note that the total contribution (7) of A and C are equal.

integration contour for all $\gamma > 0$ (shaded region). We therefore conclude that the ionisation event at zero field is a topologically stable feature of the strongly bichromatic driving field.

The counter-intuitive nature of the tunnelling without a barrier makes it highly desirable to work towards experimental realisation of this phenomenon. For this to be feasible, we need to identify an observable for which the tunnel ionisation event at zero field produces detectable signatures. Then, naturally, we strive for a comparison both with solutions to the time-dependent Schrödinger equation (TDSE) and with experimental data.

As can be seen in Fig. 4(a), the spectrum is typically dominated by orbit D which disguises the effect of B . One proposal to unveil the contribution of B is therefore to ‘remove’ D . This can be achieved by performing a colour switchover from ω to 3ω and is computationally easily modelled by neglecting the contribution of saddle point D from the summation in (6). However, even then, the tunnel ionisation event at zero field is too small to be detected in the spectrum directly.

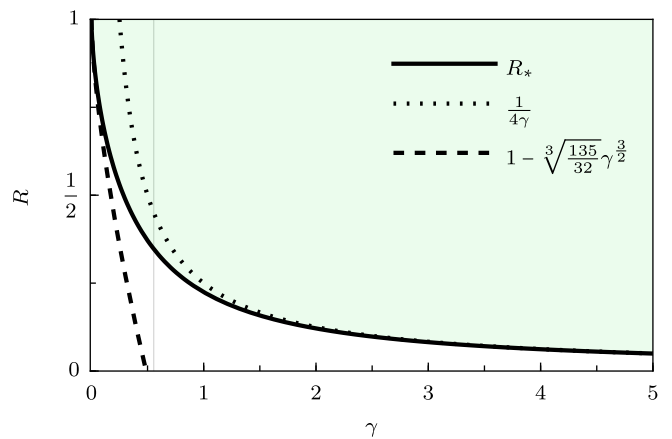


FIG. 5. Scaling of the amplitude ratio at which the saddle-point coalescence happens over a range of Keldysh parameters γ , as in Fig. 4(b). In dashed lines, asymptotes for the behaviour in the $\gamma \ll 1$ and $\gamma > 1$ regime are shown. The grey line marks the configuration used in Fig. 2, for which $\gamma = 0.67$ and the coalescence happens at $R_* \approx 0.36$.

It remains an open question for now if the event shows a signature in holographic two-dimensional interference patterns, which generally arise when using the ellipticity of the driving field to steer electron trajectories time-dependently. Moreover, whether TDSE simulations that take into account the effects of the Coulomb potential as well as the possibility of rescattering are able to isolate the contribution of the zero-field tunnelling event is still unclear. Lastly, performing a colour switchover in the driving field of HHG raises similar questions to the ones addressed here for ATI.

In conclusion, here we present strong-field tunnel ionisation events in the colour switchover from a fundamental laser field to its second harmonic. This scheme generically covers all possible two-colour fields like (4), in which the ionisation process is usually understood in terms of classically derived intuition, based on KFR theory and ultimately quasi-static assumptions. In the case of equal-amplitude mixing of the two constituent fields, we find a nonadiabatic tunnel ionisation event that happens at a time when the instantaneous electric field is zero (see Fig. 2(e)) and thereby challenges that intuitive picture of the process. The existence of the event is a topological feature of the two-colour field (4) with equal amplitudes, and has a non-zero contribution to the total spectrum from the quasi-static limit through the multiphoton regime. The classical trajectories show the need for further exploration of the under-the-barrier dynamics as well as the Coulomb effects on that specific trajectory. Moreover, although we find that the event only has a small contribution to the spectral ionisation amplitude, we expect it to play a detectable role in the heterodyne diffraction patterns of the photoelectron momentum distributions. These questions thus invite the search for an observable that provides experimentally measurable signatures of the tunnelling at zero field.

-
- [1] E. Merzbacher, The Early History of Quantum Tunneling, *Physics Today* **55**, 44 (2002).
- [2] R. Ramos, D. Spierings, I. Racicot, and A. M. Steinberg, Measurement of the time spent by a tunnelling atom within the barrier region, *Nature* **583**, 529.
- [3] D. R. Lindberg, N. Gaaloul, L. Kaplan, J. R. Williams, D. Schlippert, P. Boegel, E.-M. Rasel, and D. I. Bondar, Asymmetric tunneling of Bose–Einstein condensates, *J. Phys. B: At. Mol. Opt. Phys.* **56**, 025302.
- [4] D. M. Villeneuve, Attosecond science, *Contemporary Physics* **59**, 47 (2018).
- [5] M. Khokhlova, E. Pisanty, and A. Zaïr, Shining the shortest flashes of light on the secret life of electrons, *AP* **5**, 060501 (2023).
- [6] P. Agostini, Free-Free Transitions Following Six-Photon Ionization of Xenon Atoms, *Phys. Rev. Lett.* **42**, 1127 (1979).
- [7] W. Becker, F. Grasbon, R. Kopold, D. B. Milošević, G. G. Paulus, and H. Walther, Above-Threshold Ionization: From Classical Features to Quantum Effects, in *Advances In Atomic, Molecular, and Optical Physics*, Vol. 48, edited by B. Bederson and H. Walther (Academic Press, 2002) pp. 35–98.
- [8] P. B. Corkum, Plasma perspective on strong field multiphoton ionization, *Phys. Rev. Lett.* **71**, 1994 (1993).
- [9] K. C. Kulander, K. J. Schafer, and J. L. Krause, Dynamics of short-pulse excitation, ionization and harmonic conversion, in *Super-Intense Laser Atom Physics*, NATO Advanced Studies Institute Series B: Physics, Vol. 316, edited by B. Piraux, A. L’Huillier, and K. Rzażewski (Plenum, New York, 1993) pp. 95–110.
- [10] A.-T. Le, H. Wei, C. Jin, and C. D. Lin, Strong-field approximation and its extension for high-order harmonic generation with mid-infrared lasers, *J. Phys. B: At. Mol. Opt. Phys.* **49**, 053001 (2016).
- [11] M. Lewenstein, Theory of high-harmonic generation by low-frequency laser fields, *Phys. Rev. A* **49**, 2117 (1994).
- [12] L. Keldysh, Ionization in the field of a strong electromagnetic wave, *Sov. Phys. JETP* **20**, 1307 (1965), [*Zh. Eksp. Teor. Fiz.* **47** no. 5, p. 1945 (1965)].
- [13] F. H. M. Faisal, Multiple absorption of laser photons by atoms, *J. Phys. B: At. Mol. Phys.* **6**, L89 (1973).
- [14] H. R. Reiss, Effect of an intense electromagnetic field on a weakly bound system, *Phys. Rev. A* **22**, 1786 (1980).
- [15] A. Perelomov, V. Popov, and M. Terent’ev, Ionization of atoms in an alternating electric field: II, *Sov. Phys. JETP* **24**, 207 (1967), [*Zh. Eksp. Teor. Fiz.*, **51** no. 1, p. 309 (1967)].
- [16] R. Kopold, W. Becker, and M. Kleber, Quantum path analysis of high-order above-threshold ionization, Dedicated to Marlan O. Scully on the occasion of his 60th birthday, *Optics Communications* **179**, 39 (2000).
- [17] P. Salières, B. Carré, L. Le Déroff, F. Grasbon, G. G. Paulus, H. Walther, R. Kopold, W. Becker, D. B. Milošević, A. Sanpera, and M. Lewenstein, Feynman’s Path-Integral Approach for Intense-Laser-Atom Interactions, *Science* **292**, 902 (2001).
- [18] G. L. Yudin and M. Y. Ivanov, Nonadiabatic tunnel ionization: Looking inside a laser cycle, *Phys. Rev. A* **64**, 013409 (2001).
- [19] D. Trabert, N. Anders, S. Brennecke, M. S. Schöffler, T. Jahnke, L. P. H. Schmidt, M. Kunitski, M. Lein, R. Dörner, and S. Eckart, Nonadiabatic Strong Field Ionization of Atomic Hydrogen, *Phys. Rev. Lett.* **127**, 273201 (2021).
- [20] N. Teeny, E. Yakaboylu, H. Bauke, and C. H. Keitel, Ionization Time and Exit Momentum in Strong-Field Tunnel Ionization, *Phys. Rev. Lett.* **116**, 063003 (2016).
- [21] H. Ni, U. Saalmann, and J.-M. Rost, Tunneling exit characteristics from classical backpropagation of an ionized electron wave packet, *Phys. Rev. A* **97**, 013426 (2018).
- [22] I. Barth and O. Smirnova, Nonadiabatic tunneling in circularly polarized laser fields: Physical picture and calculations, *Phys. Rev. A* **84**, 063415 (2011).
- [23] A. S. Maxwell, A. Al-Jawahiry, T. Das, and C. F. D. M. Faria, Coulomb-corrected quantum interference in above-threshold ionization: Working towards multi-trajectory electron holography, *Phys. Rev. A* **96**, 023420 (2017).
- [24] S. A. Kelvich, W. Becker, and S. P. Goreslavski, Coulomb focusing and defocusing in above-threshold-ionization spectra produced by strong mid-IR laser pulses, *Phys. Rev. A* **93**, 033411 (2016).
- [25] P. Eckle, M. Smolarski, P. Schlup, J. Biegert, A. Staudte, M. Schöffler, H. G. Muller, R. Dörner, and U. Keller, Attosecond angular streaking, *Nature Phys* **4**, 565 (2008).
- [26] L. Torlina, F. Morales, J. Kaushal, I. Ivanov, A. Kheifets, A. Zielinski, A. Scrinzi, H. G. Muller, S. Sukiasyan, M. Ivanov, and O. Smirnova, Interpreting attoclock measurements of tunnelling times, *Nature Phys* **11**, 503 (2015).
- [27] T. Zimmermann, S. Mishra, B. R. Doran, D. F. Gordon, and A. S. Landsman, Tunneling Time and Weak Measurement in Strong Field Ionization, *Phys. Rev. Lett.* **116**, 233603 (2016).
- [28] M. Han, Unifying Tunneling Pictures of Strong-Field Ionization with an Improved Attoclock, *Phys. Rev. Lett.* **123**, 10.1103/PhysRevLett.123.073201 (2019).
- [29] M. Han, P. Ge, J. Wang, Z. Guo, Y. Fang, X. Ma, X. Yu, Y. Deng, H. J. Wörner, Q. Gong, and Y. Liu, Complete characterization of sub-Coulomb-barrier tunnelling with phase-of-phase attoclock, *Nat. Photon.* **15**, 765 (2021).
- [30] Y. Liu, W. Xie, M. Li, C. Cao, Y. Zhou, and P. Lu, Nonadiabatic tunneling ionization of atoms in few-cycle elliptically polarized laser pulses, *J. Phys. B: At. Mol. Opt. Phys.* **56**, 105601 (2023).
- [31] U. S. Sainadh, R. T. Sang, and I. V. Litvinyuk, Attoclock and the quest for tunnelling time in strong-field physics, *J. Phys. Photonics* **2**, 042002 (2020).
- [32] O. Kneller, D. Azoury, Y. Federman, M. Krüger, A. J. Uzan, G. Orenstein, B. D. Bruner, O. Smirnova, S. Patchkovskii, M. Ivanov, and N. Dudovich, A look under the tunnelling barrier via attosecond-gated interferometry, *Nat. Photon.* **16**, 304 (2022).
- [33] D. Shafir, H. Soifer, B. D. Bruner, M. Dagan, Y. Mairesse, S. Patchkovskii, M. Y. Ivanov, O. Smirnova, and N. Dudovich, Resolving the time when an electron exits a tunnelling barrier, *Nature* **485**, 343 (2012).
- [34] O. Pedatzur, G. Orenstein, V. Serbinenko, H. Soifer, B. D. Bruner, A. J. Uzan, D. S. Brambila, A. G. Harvey, L. Torlina, F. Morales, O. Smirnova, and N. Dudovich, Attosecond tunnelling interferometry, *Nature Phys* **11**, 815 (2015).
- [35] J. Zhao and M. Lein, Determination of Ionization and Tunneling Times in High-Order Harmonic Generation, *Phys. Rev. Lett.* **111**, 043901 (2013).
- [36] J. M. Dahlström, A. L’Huillier, and J. Mauritsson, Quantum mechanical approach to probing the birth of attosec-

- ond pulses using a two-colour field, *J. Phys. B: At. Mol. Opt. Phys.* **44**, 095602 (2011).
- [37] A. Fleischer, O. Kfir, T. Diskin, P. Sidorenko, and O. Cohen, Spin angular momentum and tunable polarization in high-harmonic generation, *Nature Photon* **8**, 543 (2014).
- [38] H. Eichmann, Polarization-dependent high-order two-color mixing, *Phys. Rev. A* **51**, R3414 (1995).
- [39] D. B. Milošević, Generation of circularly polarized high-order harmonics by two-color coplanar field mixing, *Phys. Rev. A* **61**, 10.1103/PhysRevA.61.063403 (2000).
- [40] M. Ivanov and E. Pisanty, Taking control of polarization, *Nature Photon* **8**, 501 (2014).
- [41] L. Medišauskas, Generating Isolated Elliptically Polarized Attosecond Pulses Using Bichromatic Counterrotating Circularly Polarized Laser Fields, *Phys. Rev. Lett.* **115**, 10.1103/PhysRevLett.115.153001 (2015).
- [42] S. V. Popruzhenko, Keldysh theory of strong field ionization: History, applications, difficulties and perspectives, *J. Phys. B: At. Mol. Opt. Phys.* **47**, 204001 (2014).
- [43] G. B. Arfken, H.-J. Weber, and F. E. Harris, *Mathematical Methods for Physicists: A Comprehensive Guide*, 7th ed. (Elsevier, 2013).
- [44] O. Smirnova and M. Ivanov, Multielectron High Harmonic Generation: Simple man on a complex plane, in *Attosecond and XUV Physics: Ultrafast Dynamics and Spectroscopy*, edited by T. Schultz and M. Vrakking (John Wiley & Sons, 2013).
- [45] A. Nayak, M. Dumergue, S. Kühn, S. Mondal, T. Csizmadia, N. G. Harshitha, M. Füle, M. Upadhyay Kahaly, B. Farkas, B. Major, V. Szaszko-Bogár, P. Földi, S. Majorosi, N. Tsatrafyllis, E. Skantzakis, L. Neoričić, M. Shirozhan, G. Vampa, K. Varjú, P. Tzallas, G. Sansone, D. Charalambidis, and S. Kahaly, Saddle point approaches in strong field physics and generation of attosecond pulses, *Physics Reports* **833**, 1 (2019).
- [46] N. Bleistein and R. A. Handelsman, *Asymptotic Expansions of Integrals* (Arden Media, 1975).
- [47] E. Pisanty and M. Ivanov, Slalom in complex time: Emergence of low-energy structures in tunnel ionization via complex-time contours, *Phys. Rev. A* **93**, 043408 (2016).
- [48] L. Torlina and O. Smirnova, Time-dependent analytical R -matrix approach for strong-field dynamics. I. One-electron systems, *Phys. Rev. A* **86**, 043408 (2012).